

Cite this: *Soft Matter*, 2011, **7**, 9012

www.rsc.org/softmatter

PAPER

Free energy analysis of vesicle-to-bicelle transformation†

Wataru Shinoda,^{*ab} Takenobu Nakamura^{ab} and Steven O. Nielsen^c

Received 8th March 2011, Accepted 20th June 2011

DOI: 10.1039/c1sm05404j

A lipid assembly composed of a finite number of lipid molecules can have multiple metastable structures. Using a series of coarse-grained molecular dynamics simulations, we evaluate the free energy profile for the transformation of a small vesicle to a disk-like structure called a bicelle. This free energy is found to be lower than that predicted from continuum elastic theory. For small unilamellar vesicles, the relaxation of the internal structure of the membrane is suggested to play an important role in lowering the free energy barrier for the vesicle-to-bicelle transformation.

1 Introduction

A lipid self-assembly generally shows polymorphism depending on the concentration and thermodynamic conditions.¹ A primitive understanding of the morphology of lipid self-assembly has been made by the shape of the lipid molecules based on a critical packing parameter,² though it is, in general, nontrivial to understand the phase diagram from a molecular viewpoint even if we limit our discussion to the bilayer-forming lipids. Furthermore, a determination of the phase boundary could be occasionally difficult due to the coexistence of phase structures and also sometimes due to the hysteresis or long-time relaxation of the structure. These complex systems often show metastability due to an inherent rugged free energy landscape. This is a major obstacle for us to understand and to control the phase structure. Phenomenological continuum elastic theory based on simple expressions for the curvature energy has been foundational in gaining a qualitative physical understanding of lipid assemblies and especially the energetics of lipid membrane transformations.^{3,4} These approaches shed light on which properties are important to characterize the observed membrane morphology on the continuum model level. However, continuum approaches have difficulties describing topological changes such as happen during pore formation in a membrane, and are limited by simplifying assumptions required for the resulting equations. In contrast, computer simulations are free of these limitations and can be used to study a wide range of membrane processes at the molecular scale.⁵ They provide the ability to do ‘experiments’

in a controlled manner at molecular resolution, and the resulting data can be used to gain understanding into nanoscale phenomena and to conduct stringent tests of the elastic theory predictions.

Indeed, molecular simulations would be expected to be useful to predict the morphology changes from a molecular viewpoint but have been of limited use due to difficulty in achieving the relevant spatial or temporal scales. This difficulty can be overcome through the use of coarse-grained (CG) molecular models, which can now access systems containing a small vesicle made by several thousands of lipid molecules. CG models, which are constructed based on fully atomistic molecular dynamics (AA-MD) analysis, provide a reasonable description of several important physical quantities including surface tension, density, and solvation free energy as well as structural properties such as the equilibrium area per lipid and the electron density normal to the membrane plane.⁶ Encouraged by this success, we have applied CG-MD to studies of lipids, surfactants, colloids, and peptides.^{6–12} Furthermore, it has been shown that the CG model produces reasonable elastic properties for planar lipid membranes such as the area expansion and bending moduli.⁶

Thus, CG-MD can now be used to assess the properties of curved membranes and then to provide useful information to evaluate the assumptions made in phenomenological continuum theory. To achieve this aim, however, we still need a strategy to evaluate the free energy due to the morphology change of molecular assemblies. This article presents our trial to assess the free energy of a lipid assembly during a vesicle-to-bicelle transformation.

In our recent CG-MD paper,⁶ it has been shown that lipid assemblies randomly generated with 1,2-dimyristoyl phosphatidylcholine (DMPC) molecules transform into a bicelle or a vesicle, depending on the size, *i.e.*, the number of DMPC molecules. No other structure is found to be stable during 1 μ s CG-MD simulations. Vesicle formation was observed only for the lipid aggregates with more than 1512 DMPC molecules. This observation is well explained by a simple phenomenological model proposed by Fromherz,³ where the vesicle-to-bicelle

^aNanosystem Research Institute, National Institute of Advanced Industrial Science and Technology (AIST), Central 2, Umezono 1-1-1, Tsukuba, 305-8568, Japan. E-mail: w.shinoda@aist.go.jp; Fax: +81 29 851 5426; Tel: +81 29 861 6251

^bCREST, Japan Science and Technology Agency (JST), 4-1-8 Honcho, Kawaguchi, Saitama, 332-0012, Japan

^cDepartment of Chemistry, The University of Texas at Dallas, 800 West Campbell Road, Richardson, Texas, 75080, USA

† Electric supplementary information (ESI) available: See DOI: 10.1039/c1sm05404j

morphology change is characterized by two free energy contributions: the free energy at the bilayer edge and the membrane bending free energy. The former is known as a line tension term that describes the free energy cost due to the lipid reorientation and conformational changes at the bilayer edge, while the latter is the free energy cost due to the bending of the bilayer membrane whose spontaneous curvature is zero. The larger the aggregate size, the larger the line tension term becomes while the free energy cost due to membrane bending becomes smaller due to the increased radius of the vesicle morphology. Fromherz described the free energy as a function of an order parameter assuming a constant membrane area and a (fragment of a) spherical shape for the partially formed vesicle. These assumptions are found to be reasonable in examining our previous CG-MD results.⁶ As an example, a transformation of a lipid aggregate made by 1512 DMPC molecules in a dilute aqueous solution is given in Fig. 1. The initial aggregate structure was randomly generated (see ref. 6 for the details). Within 10 ns, the aggregate eliminated the defects in the bilayer membrane and transformed into a fragment of a spherical vesicle. It took 100–200 ns for the vesicle to seal into a closed form, though the actual timing of the process depended on the initial configuration. During the transformation, the aggregate kept the shape of a spherical vesicle fragment by exchanging lipids between the inner and outer leaflets to go along a supposed free energy local minimum pathway. Since the lipid exchange (flip-flop) occurred only at the bilayer edge, the vesicle formation process slowed down in its later stages due to the limited bilayer edge length, and thus a small pore in the vesicle was found to persist for a long time (more than 50 ns) at the final stage of the vesicle formation. Although the lipid motions were completely ignored in the Fromherz theory, where the membrane is assumed to be an elastic sheet with zero thickness, the theory successfully characterizes the overall features of even small lipid

aggregates. For example, the theory predicts that there is a parameter range in which two local minima in the free energy of the lipid aggregate exist, corresponding to the bicelle and vesicle structures. This was confirmed by CG-MD of 1512 DMPC molecules; as discussed above, a spontaneous vesicle formation was observed for a randomly generated aggregate with 1512 DMPC molecules, while the prepared bicelle with the same number of DMPC molecules also appeared to be stable and did not show any sign of transforming to a closed vesicle during 700 ns of CG-MD.⁶ This observation motivated us to investigate how well such a continuum theory characterizes the behavior of a small aggregate where the membrane thickness is comparable to the inner radius of the closed vesicle.

In the present paper, we calculated the free energy cost to open a mouth in a small vesicle. We used the small vesicle made by 1512 DMPC molecules, which showed bistability as a closed vesicle or a bicelle (flat disk). By opening a mouth in the DMPC vesicle, we found it eventually transformed into a bicelle during a series of CG-MD simulations. To make a rigorous comparison with the Fromherz theory, we also estimated the line tension from the pore formation free energy of the corresponding planar membrane and evaluated the Gaussian curvature modulus using an analysis of the stress profile across the membrane. Finally we discuss the discrepancy between the Fromherz theory and our CG-MD data with respect to the free energy barrier for the vesicle-to-bicelle transformation.

2 Theory and computational methods

2.1 Model, system setting and molecular dynamics simulations

We used the recently developed CG model of a DMPC lipid membrane in aqueous solution.^{6–8} A DMPC molecule is

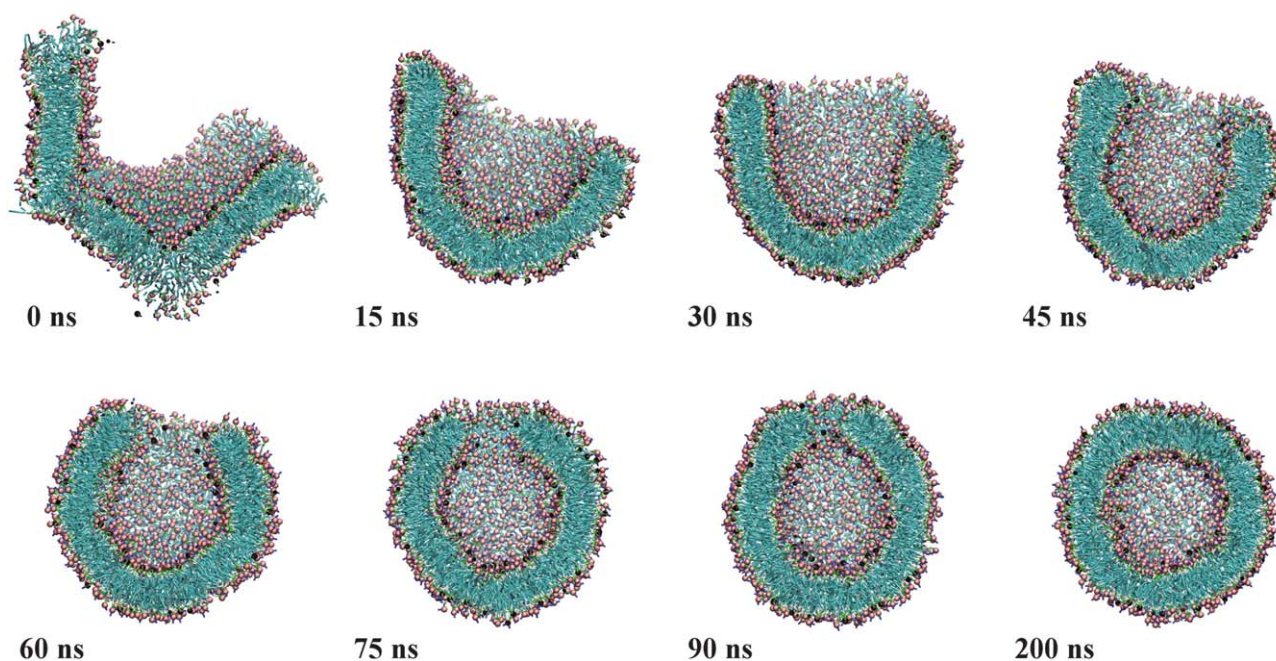


Fig. 1 A series of cross-sectional views of a lipid aggregate during a CG-MD simulation from an arbitrarily generated initial configuration with 1512 DMPC molecules in a dilute aqueous solution. Hydrophobic tails are drawn in cyan with lines, while hydrophilic phosphate groups are drawn with red spheres. Water particles are eliminated for clarity.

represented by 13 CG sites connected by harmonic bond and bond angle potentials to produce a molecular configuration consistent with AA-MD results. Water CG particles are treated explicitly, though each one represents three water molecules. Density, surface/interfacial tension, and solvation free energy are the target properties against which the non-bonded parameters of the CG model are optimized. The lipid membrane molecular area, repeat spacing, and order parameter profile are accurately captured by the CG model. For further details we refer interested readers to our previous paper.⁶

A vesicle system was constructed in a simulation box with 1512 DMPC lipids and hydrated with 100 CG water particles (effectively 300 water molecules) per DMPC molecule. The initial configuration was taken from our previous MD study of the same system where a spontaneous vesicle formation was observed from a randomly generated lipid aggregate.⁶ The formation of a closed vesicle took typically 100–200 ns, which depends on the initial configuration of the lipid molecules, though the structure of the resulting vesicle is more or less invariant: the number of lipids in the inner and outer leaflets are about 510 and 1000, respectively, with an uncertainty of less than 10 lipid molecules. After the formation of a closed vesicle, no flip-flop motion was observed over an additional 1 μ s simulation.

A series of CG-MD simulations of a planar DMPC membrane system has also been conducted to compute the pore formation free energy and the line tension of the membrane. The planar bilayer system consists of 1152 DMPC molecules and 33057 CG water particles, which corresponds to about 86 water molecules per lipid. This corresponds to a much higher hydration state than the fully hydrated multilamellar phase¹³ and is necessary to avoid artifacts caused by the shrinking inter-membrane spacing which occurs as the pore is widened (see supplementary materials for details).

All MD simulations have been carried out in the NPT ensemble with three-dimensional periodic boundary conditions (PBC). The temperature of 310 K was controlled using the Nosé–Hoover chain method (length = 5).¹⁴ The pressure of 0.1 MPa was controlled using an Andersen isotropic barostat for the vesicle system, while semi-isotropic coupling to a Parrinello–Rahman barostat was chosen for the planar membrane case.^{15–17} The reversible RESPA algorithm was used to integrate the equations of motion with two different time steps. The long time step of 40 fs is used to update the forces from the long-range nonbonded interactions including the reciprocal space contribution of the Ewald sum and real space contribution from particles at a distance of longer than 0.81 nm, while the short time step of 5 fs is used to update all the remaining forces such as the short-range nonbonded interactions and all bonded interactions. The Coulomb interaction is computed using the Ewald sum.¹⁸ All MD simulations have been carried out using our in-house simulation software package, MPDyn.^{19,20}

2.2 Fromherz model

A phenomenological description of vesicle stability was proposed by Fromherz.³ In this model, the Gibbs free energy of a fluid membrane spherical fragment is used to characterize the stability during a vesicle-to-bicelle morphology transformation.

Assuming a constant membrane area (in this elastic theory model the membrane has a zero thickness) and composition during the morphology change, the transformation free energy is proposed to consist of two competing contributions: the free energy at the bilayer edge and the membrane bending free energy

$$G = \frac{1}{2} \left(\kappa_c + \frac{1}{2} \bar{\kappa} \right) \left(\frac{2}{\rho} \right)^2 A + \gamma_l l \quad (1)$$

where κ_c and $\bar{\kappa}$ are the mean curvature and Gaussian curvature moduli, respectively, and γ_l is the line tension. ρ is the radius of the sphere on which the membrane fragment is constrained and l is the edge length of the membrane fragment. The area of the membrane fragment, A , is kept constant so that the edge length l is changed as a function of the curvature $1/\rho$.

2.3 Free energy calculations

We evaluate the free energy to open a pore in curved and planar membranes made by DMPC lipid molecules. The thermodynamic integration (TI) method was used to compute the free energy profile along the reaction path. We introduced a bias potential (wall potential) to make a pore in the membranes;

$$U(d) = \begin{cases} -\frac{1}{3}kd^3, & (d \leq 0) \\ 0, & (d > 0) \end{cases} \quad (2)$$

where d is the signed length of the normal vector of the wall surface pointing outward from the closest point of the wall surface to the particle position. A negative value of d means that the particle has penetrated inside the wall. k is the force constant, which can be arbitrarily chosen but should be large enough to clearly give the expected deformation (pore formation) of the membrane. We selected a cubic potential energy function to remove the discontinuity in the second derivative at $d = 0$ that would have occurred had a harmonic potential been chosen.

For the planar membrane, we employed a cylindrical wall potential with the axis taken along the bilayer normal, z . In this case, the wall potential is

$$U(r_{i,xy}, R) = \begin{cases} -\frac{1}{3}k(r_{i,xy} - R)^3, & (r_{i,xy} \leq R) \\ 0, & (r_{i,xy} > R) \end{cases} \quad (3)$$

where R is the radius of the cylinder and $r_{i,xy} = \sqrt{x_i^2 + y_i^2}$ is the distance of particle i from the central axis of the cylinder. From eqn (3), a particle i is expelled only from the cylindrical region of radius R and does not feel any external force outside of this region. We apply the bias potential only to the hydrophobic tails of lipid molecules so that water and lipid headgroups are free to move across the cylindrical region with no energetic penalty. Thus, in a sense, the pore is made in the hydrophobic core of the membrane. By changing the radius of the cylinder gradually, we can measure the free energy change due to the pore formation in a planar lipid membrane. To use the TI method, we carried out a series of CG-MD simulations using different R values in eqn (3), and in each case measured the average force acting on the cylindrical wall.²¹ Namely, to increase the cylinder radius from zero to R , the system free energy is calculated from,

$$\begin{aligned}
 \Delta G(R) &= \int_0^R \left\langle \left(\sum_i \frac{\partial U(r_{i,xy}, R')}{\partial R'} + \frac{\partial PV}{\partial R'} \right) \right\rangle dR' \\
 &= \int_0^R \left\langle \sum_i \frac{\partial U(r_{i,xy}, R')}{\partial R'} \right\rangle dR' + P\langle \Delta V \rangle \\
 &\approx \int_0^R \left\langle \sum_i \frac{\partial U(r_{i,xy}, R')}{\partial R'} \right\rangle dR' \\
 &= \int_0^R \left\langle \sum_{i, (r_{i,xy} < R)} k(r_{i,xy} - R')^2 \right\rangle dR'
 \end{aligned} \tag{4}$$

where $\langle \dots \rangle$ represents the NPT ensemble average. The second term has a non-zero contribution, though its value is found to be much smaller than the statistical error of the first term; *e.g.*, $P\langle \Delta V \rangle = P(\langle V(R) \rangle - \langle V(0) \rangle)$ is about 0.04 kJ mol^{-1} even at $R = 4 \text{ nm}$. Thus, we ignore the $P\langle \Delta V \rangle$ term and compute the free energy change due to the external cylindrical bias potential by conducting the integration in eqn (4). To obtain a reasonable estimation of the free energy change, we chose the sampling points as $R = 0.1, 0.2, 0.3, 0.4, 0.5, 0.6, 0.8, 1.0, 1.2, 1.4, 1.6, 1.8, 2.0, 2.4, 2.8, 3.2, 3.6,$ and 4.0 nm , respectively. At each sampling point, we have carried out a CG-MD run for 100–150 ns to see an adequate convergence of the potential of mean force (PMF). The free energy $\Delta G(\mathcal{R})$ to make a pore of radius \mathcal{R} is not exactly that of eqn (4) because the actual radius of the pore, \mathcal{R} , is slightly shifted from R of the cylindrical wall potential. In other words, the free energy computed from eqn (4) depends on the choice of the force constant, k . We can eliminate the k dependency of the free energy change by taking the reaction coordinate as \mathcal{R} instead of R .

In the actual computation, \mathcal{R} is not controlled but rather is computed from the density profile of the hydrophobic core of the membrane along the radial cylinder direction, $\rho_c(R')$. We define \mathcal{R} as the minimum radius where $\rho_c(R')$ has a non-zero value. Although the choice of the force constant k does affect $\langle \partial U / \partial R \rangle$, plotting ΔG as a function of \mathcal{R} eliminates the dependency of the free energy on k , allowing for an arbitrary choice of k . We chose a rather large value of $k = 4.184 \times 10^6 \text{ kJ mol}^{-1} \text{ nm}^{-3}$ ($=1000 \text{ kcal mol}^{-1} \text{ \AA}^{-3}$) in our free energy (FE) calculations, though we confirmed that $k = 4.184 \times 10^5 \text{ kJ mol}^{-1} \text{ nm}^{-3}$ ($=100 \text{ kcal mol}^{-1} \text{ \AA}^{-3}$) gave the same free energy profile as a function of \mathcal{R} (see supplementary materials for details). The choice of a large k gives a minor difference between R and \mathcal{R} ; $\mathcal{R} - R \approx -0.02 \text{ nm}$. Note that we assume that the pore is circular when using the cylindrical bias potential. This may not always be reasonable especially when the pore is very small. However, the main purpose of this free energy analysis for the planar membrane is to obtain the line tension at the bilayer edge, which is given as the slope of the free energy change as a function of the edge length. For this purpose, we can just focus on the PMF for large values of R , *i.e.*, the integrand of eqn (4). Further details will be given in the results section.

For the curved membrane system, we used a wall potential with a conical shape to open the vesicle as shown in Fig. 2. We again used the bias potential as defined in eqn (2). We place the cone vertex at $(0, 0, Z_c)$ and point the cone along the z axis with a vertical angle of θ . The force exerted on a particle i in the region $d \leq 0$ is computed as,

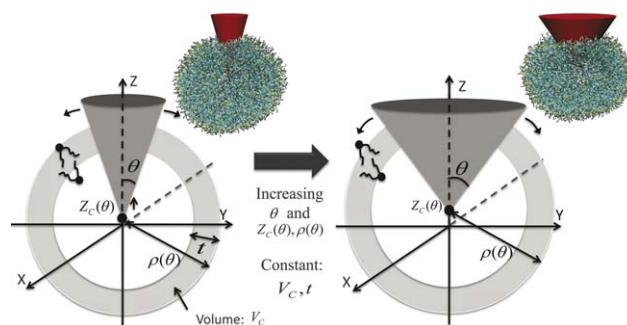


Fig. 2 Images of the operation to open the vesicle using a conical bias potential. The center of mass of the lipids is kept at the origin by applying a harmonic constraint. Due to the lipid mass removed from the cone interior, this center of mass does not coincide with the center of the sphere containing the opened vesicle spherical fragment. The sphere center, which is also the vertex of the cone, gradually shifts upwards as the cone angle θ increases. The vesicle hydrophobic shell is drawn in light grey. Actual snapshots from the CG-MD runs, with the bias potential shown in red, are given on the shoulder of each schematic picture.

$$F_{i,x} = kd^2 \frac{x_i}{\sqrt{x_i^2 + y_i^2}} \cos \theta, \tag{5}$$

$$F_{i,y} = kd^2 \frac{y_i}{\sqrt{x_i^2 + y_i^2}} \cos \theta, \tag{6}$$

$$F_{i,z} = -kd^2 \sin \theta. \tag{7}$$

It is clear from these equations that the bias potential pushes the particles downward along the z -axis. Namely, in a long CG-MD simulation, the bias potential can eventually push the entire vesicle out of the range of the cone potential. This means that we need an additional restraint to open a vesicle with the cone potential. Thus, we also apply a harmonic bias to constrain the center of mass of the lipids to the origin (the center of simulation box). Note that this harmonic constraint, applied without the cone bias potential, does not perform any work on the system. This second constraint, combined with the removal of lipids from the cone mouth due to the cone potential, means that the center of mass of the lipids does *not* coincide with the center of the sphere of which the lipids form a spherical fragment (see Fig. 2). The center of the sphere clearly depends on θ and coincides with the cone vertex; we can calculate Z_c as

$$Z_c = \frac{\pi}{4V_c} \sin^2 \theta \left\{ \rho(\theta)^4 - (\rho(\theta) - t)^4 \right\} \tag{8}$$

where V_c is the volume of the membrane hydrophobic core, $\rho(\theta)$ is the outer radius of the hydrophobic shell of the vesicle fragment, and t is the thickness of the hydrophobic layer of the membrane. To obtain this expression we have assumed that the lipid aggregate morphology is a spherical fragment as assumed by Fromherz and as seen qualitatively in Fig. 1. In addition, we have assumed that the volume and thickness of the membrane hydrophobic core do not change during the transformation, which implies that the membrane area is invariant as assumed in the Fromherz model.³ V_c , t , and $\rho(0)$ are estimated from MD trajectories of the closed vesicle. $\rho(\theta)$ is computed based on the constant volume assumption, *i.e.*, by solving the relation

$$\frac{2}{3}\pi\{\rho(\theta)^3 - (\rho(\theta) - t)^3\}(1 + \cos\theta) = V_C. \quad (9)$$

The reaction coordinate for this free energy analysis is the vertex angle of the opened cone, θ_p . Similar to the case of the cylinder wall, θ_p is not exactly the same as θ . Again ignoring the $P\langle\Delta V\rangle$ term, the free energy due to opening the pore in the vesicle should be written as,

$$\begin{aligned} \Delta G(\theta_p) &\approx \int_0^{\theta_p} \left\langle \sum_i \frac{\partial U(r_i, \theta)}{\partial \theta_p} \right\rangle d\theta_p' \\ &= \int_0^{\theta_p} \left\langle \sum_i \frac{\partial U(r_i, \theta)}{\partial \theta} \left(\frac{\partial \theta}{\partial \theta_p} \right) \right\rangle d\theta_p' \\ &\approx \int_0^{\theta_p} \left\langle \sum_i \frac{\partial U(r_i, \theta)}{\partial \theta} \right\rangle d\theta \\ &= \int_0^{\theta_p} \left\langle \sum_{i, (d \neq 0)} k d^2 \{ \sqrt{x_i^2 + y_i^2} \sin \theta \right. \\ &\quad \left. + (z_i - Z_C) \cos \theta \} + k_{\text{COM}} |\mathbf{R}_{\text{COM}}| \right\rangle d\theta \end{aligned} \quad (10)$$

In the third line, we assumed $(\partial\theta/\partial\theta_p) \approx 1$. This approximation is reasonable when we use $k = 4.184 \times 10^6 \text{ kJ mol}^{-1} \text{ nm}^{-3}$ ($=1000 \text{ kcal mol}^{-1} \text{ \AA}^{-3}$). In principle, we can evaluate $(\partial\theta/\partial\theta_p)$ from the density profile of the hydrophobic shell of the vesicle fragment as done for the planar membrane. However, an opened vesicle can show rather large fluctuations in its shape which results in significant noise and makes it difficult to determine the actual opened vertex angle, θ_p , precisely. Therefore, we approximate $(\partial\theta/\partial\theta_p) \approx 1$ by choosing a large force constant for the wall potential. As found in the planar membrane, the uncertainty of the reaction coordinate due to this approximation should be quite minor with our choice of force constant, k . The PMF sampling was made using a 100 ns CG-MD simulation at each fixed point of θ of 1, 2, 3, 4, 5, 6, 7, 8, 9, 10, 12, 14, 16, 18, 20, 22, 24, 26, 28, 30, 32, 34, 36, 38, 40, 45, 50, 55, 60, 65, 70, 75, 80, 85, and 90 degrees, respectively, even though the convergence of the PMF was not obtained for $\theta > 65$ –70 degrees as mentioned later.

2.4 Gaussian curvature modulus

We evaluate the Gaussian curvature modulus using the second moment of the stress profile along the bilayer normal.²²

$$\bar{\kappa} = \int_{-D/2}^{D/2} \pi(z) z^2 dz \quad (11)$$

where $\pi(z)$ is the lateral pressure profile along the bilayer normal, z , which is computed from the difference between the lateral and normal components of the pressure profile;

$$\pi(z) = P_L(z) - P_N(z). \quad (12)$$

In the notation of eqn (11), the origin of the z -axis was chosen at the bilayer center, which is regarded as the pivotal plane of the bilayer membrane. We used a rather small membrane patch composed of 128 DMPC lipids with 2050 CG water particles to compute the stress profile. D was set to 6 nm, which is large enough to span the membrane. We evaluated the stress profile using two different integration contours, namely the Irving–Kirkwood (IK) and Harashima (H) contours, respectively,

following the method proposed by Sonne *et al.*²³ The Ewald sum was used to evaluate the stress profile when the H contour was used, while an electrostatic cutoff scheme was used with the IK contour due to the limitation of the method. However, the stress profile using a cutoff of 1.5 nm already gives a reasonable convergence and hardly any deviation is detected by changing the cutoff to 2.5 nm. Thus, we chose the latter safely when using the IK contour. Note that the cutoff length of the LJ terms in the CG model is fixed at 1.5 nm as determined in the original paper.⁶

3 Results

3.1 Planar membrane

Fig. 3(a) plots the free energy change due to pore formation in the planar membrane as a function of the pore radius. The free energy rapidly increases for small pore radii, though it changes linearly with the radius for larger pores of $\mathcal{R} > \sim 1.5$ nm. The slope of the linear regime gives the line tension of the membrane, which is defined as the derivative of the free energy change with respect to the length of the bilayer rim, $l = 2\pi\mathcal{R}$.

$$\frac{dG}{dl} = \frac{1}{2\pi} \left(\frac{dG}{d\mathcal{R}} \right) \approx \frac{1}{2\pi} \left\langle \frac{\partial U}{\partial \mathcal{R}} \right\rangle. \quad (13)$$

The plot of (dG/dl) as a function of \mathcal{R} is given in Fig. 3(b). As mentioned above, the approximated expression in eqn (13), where U is given in eqn (3), is quite accurate for large values of \mathcal{R}

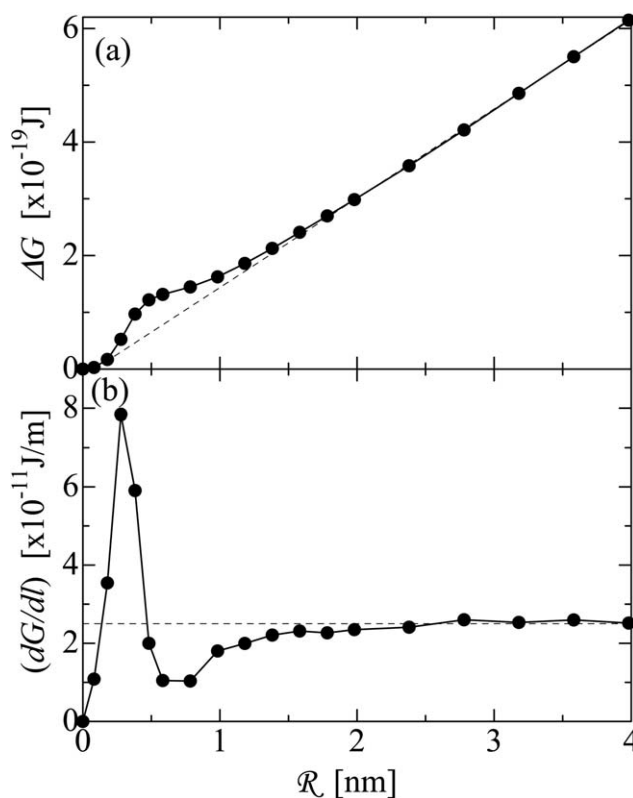


Fig. 3 (a) Pore formation free energy in the planar DMPC bilayer as a function of the pore radius. (b) The scaled potential mean force, (dG/dl) , as a function of the pore radius. The error bars are smaller than the symbols.

because it reaches a plateau value. The quantity $\langle \partial U / \partial R \rangle$ in eqn (13) is the mean force, which is directly computed during a fixed- R CG-MD run, and is precisely the integrand in the last line of eqn (4). Since (dG/dl) converges to a finite value regardless of the force constant, k , or \mathcal{R} , as long as $\mathcal{R} > 1.5$ nm, we can evaluate the line tension accurately.

A 100 ns NPT-MD simulation has been carried out for each cylinder radius to obtain well converged PMF values. The line tension was estimated as 25 ± 2 pN. The calculated line tension is well in the range of the experimental values, 5 to 50 pN, for similar PC membranes, though the line tension seems a nontrivial quantity to be determined experimentally.^{24–31} An evaluation of the line tension using atomistic MD simulations was reported by computing the average pressure anisotropy of DMPC ribbon systems, and yielded the value of 10 to 30 pN.³² Our estimation is again well within these bounds.

In order to obtain an accurate estimation of the line tension using our method, we need a thick water layer to eliminate the energy contribution from the inter-bilayer interaction, which comes through the PBC employed in our MD simulations. By increasing the radius of the cylindrical wall potential, the effective inter-bilayer distance is shortened due to the PBC. Therefore, we introduced plenty of water particles to make a water layer with a thickness of about 10 nm in the intact membrane system. Using a thin water layer, we found a non-linear slope for large \mathcal{R} values in the free energy plot due to the contribution from the inter-bilayer interaction (see supplementary materials).

It should be noted here that the computation of the line tension is independent of the choice of the force constant, k , in the repulsive cylindrical potential. All that is needed is to run a MD simulation long enough to obtain a well converged PMF at large pore radii (Fig. 3(b)). Furthermore, just to obtain the line tension, we can carry out only a single CG-MD run and measure the PMF in eqn (13) at a large value of \mathcal{R} . The convergence of the PMF is excellent after 100 ns CG-MD as seen in Fig. 3. This must be advantageous over the previously reported method based on the pressure computation of lipid ribbon systems.³²

For small pore radii we found a significant deviation in the free energy from a linear function. This is again evident from Fig. 3(b). A rapid growth of the free energy at small radii is due to the hydrophobic nature of the small pore. When the pore is small, lipid molecules are just displaced laterally without changing their orientation. The pore is, however, large enough to contain water molecules so that the hydrophobic tails of the lipids are exposed to water. For pores with radii of ≥ 0.5 nm, however, the lipids around the rim of the bilayer start to reorient to minimize the exposure of their hydrophobic tails to the pore region. Fig. 4 shows a snapshot from a MD run with the cylindrical bias potential of 1 nm in the radius. At this stage, the DMPC lipids at the rim reorient to cover the bilayer edge with their headgroups. This local structural rearrangement of lipids initiated at the pore radius of around 0.5 nm is completed at around 1.5 nm. For pores with a radius larger than about 1.5 nm, it should be reasonable to expect the molecular structure at the bilayer rim to be more or less the same, because the free energy becomes a simple function of the line length. Similar lipid reorientations were previously detected by atomistic MD simulations.³³

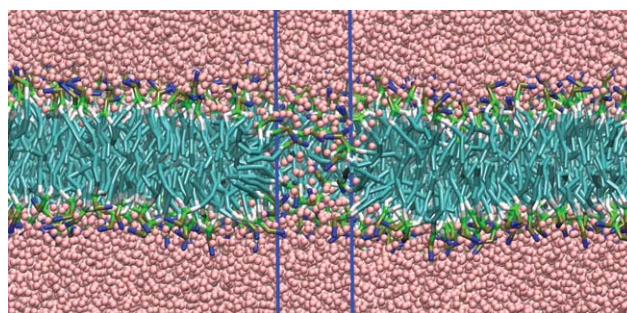


Fig. 4 A snapshot of a planar DMPC lipid bilayer in the presence of a cylindrical bias potential with a radius of 1 nm. Hydrophobic tails, ester groups, glycerols, phosphates, and cholines are drawn in cyan, white, green, tan, and blue, respectively. Pink particles denote water CG particles.

3.2 Vesicle

Now we turn our attention to the free energy required to open a vesicle. Fig. 5 plots the free energy needed to open a closed vesicle composed of 1512 DMPC molecules using a conical bias potential. Similar to the planar case, we detect a rapid increase of free energy for small vertex angles. The mechanism responsible for the small-vertex features in the free energy curve is more or less the same as in the planar membrane case; namely, the pore changes from hydrophobic to hydrophilic due to the re-orientation of the DMPC lipids around the bilayer edge. Further growth of the pore for vertex angles of >5 degrees is still unfavorable, though the free energy cost to increase the pore size in the vesicle is not as large as that in the planar bilayer. This is because the free energy cost due to membrane bending is reduced by changing the mean curvature of the membrane during the opening of the vesicle. Due to the bending free energy contribution, the vesicle free energy does not simply grow as the vertex angle increases and eventually acquires a negative slope. However, we cannot quantify the decrease of free energy, because our measurement of the PMF is just a one-way opposed

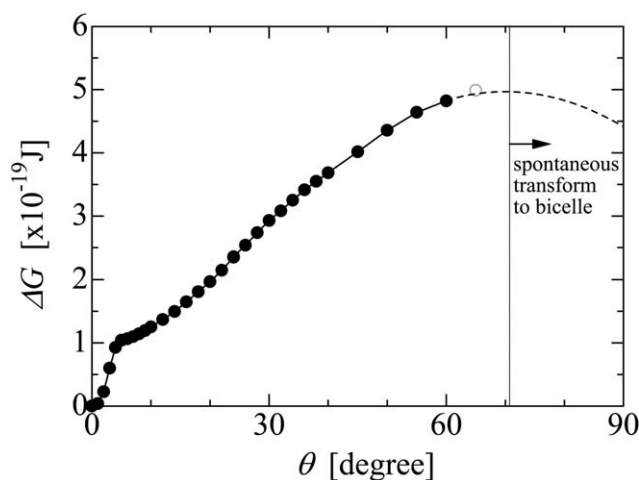


Fig. 5 Free energy change of opening a vesicle as a function of the vertex angle of the conical bias potential. The error bars are smaller than the symbols.

force due to the purely repulsive nature of the cone potential. This means that the PMF is accurate where the free energy increases rapidly (the smaller vertex angles), and becomes less accurate where the free energy change is slow (the larger vertex angles). For the latter case, we observed a larger fluctuation of the vesicle edge so that it took more time to see the convergence of the PMF. During the constrained MD run with the biasing cone potential at $\theta = 75^\circ$, a spontaneous transformation to the disk-like bicelle structure was observed as shown in Fig. 6. This suggests that the peak of the free energy barrier for the vesicle-to-bicelle transformation is located below $\theta = 75^\circ$. Actually the mean forces at $\theta = 65$ and 70 degrees are very small and do not converge well even with 100 ns of constrained MD, because in these cases the lipid assembly hardly touched the cone wall. Based on these observations an approximate extrapolation was made as the dashed line in Fig. 5. This extrapolation suggests that the free energy barrier for the vesicle-to-bicelle transition is about 5×10^{-19} J for this small vesicle composed of 1512 DMPC molecules.

3.3 Stress profile across the planar membrane and Gaussian curvature modulus

In order to evaluate the Gaussian curvature modulus, we computed the pressure profile across a planar DMPC bilayer membrane. Fig. 7 plots the pressure profiles across the membrane using two different integration contours; namely the IK and H contours, respectively. The pressure profiles were well converged using 100 ns CG-MD trajectories. The symmetry of the measured pressure profiles with respect to the bilayer central plane demonstrates the excellent convergence. Although Sonne *et al.* suggested that the computed pressure profile hardly depends on the choice of contour, this may be due to the large statistical error in their AA simulations resulting from a limited simulation time length. We clearly observe a nontrivial dependence on the contour as seen in Fig. 7. Moreover, as mentioned in the methods section, we did not detect a notable change in a given pressure profile as long as we used a cutoff distance for the Coulomb interactions longer than 1.5 nm. Therefore the treatment of the long-range Coulomb interactions does not account for the discrepancy in these two profiles. Using eqn (11), we obtained the Gaussian curvature modulus, $\bar{\kappa}$, as -4.59×10^{-20} J with the IK contour and -2.62×10^{-20} J with the H contour. Thus, the choice of the contour results in a significant difference even in the Gaussian curvature modulus. The Gaussian curvature modulus is known to have a negative value as found in our estimation. The H contour was previously found to be problematic when it was used in spherical coordinates, showing that the pressure depended on the distance from the

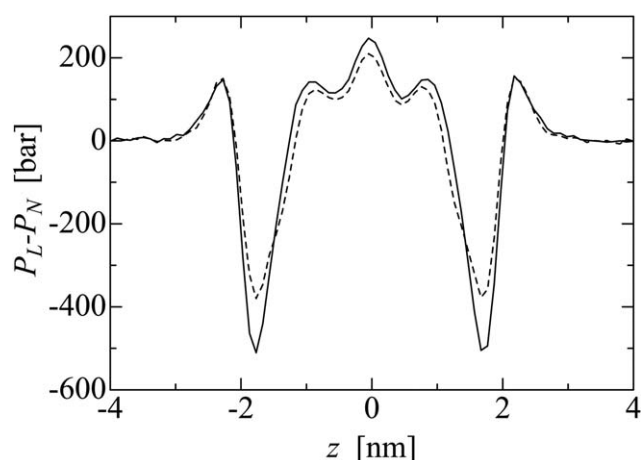


Fig. 7 Stress profile across the planar DMPC bilayer membrane. The origin of the z axis is taken at the central plane of the bilayer. Solid line: Irving–Kirkwood integration contour using the truncation of the Coulomb interaction at 2.5 nm. Dashed line: Harashima integration contour with the Ewald sum for the Coulomb interaction.

origin,³⁴ though the H contour showed no clear failure in Cartesian coordinates. Although the pressure profile has often been used to characterize the mechanical properties of lipid membranes from MD simulations, not much attention has been paid to the choice of contour.

4 Discussion

For the vesicle-to-bicelle transformation, the reaction path we selected is not the only choice. However, as shown in Fig. 1, the pathway for spontaneous vesicle formation from a random lipid aggregate typically occurs by way of a bowl-like structure, which is well described as a spherical fragment. This is commonly observed for any size of lipid aggregate as long as a spontaneous vesicle formation was observed.⁶ In addition, it is a reasonable assumption that, from the viewpoint of the energy cost at the bilayer rim, the circular mouth made by the cone bias potential gives a vesicle-to-bicelle transition pathway with the minimal free energy cost.

It would be valuable to compare the vesicle-opening free energies obtained from CG-MD and Fromherz's theory. Fig. 8 plots the pore formation free energy in a planar membrane and a vesicle as obtained from CG-MD as a function of the line length at the bilayer rim. The line length of the bilayer rim in the vesicle was not directly measured from the MD trajectory, but was computed with the assumption of a spherical fragment geometry during the transformation pathway. Also the line

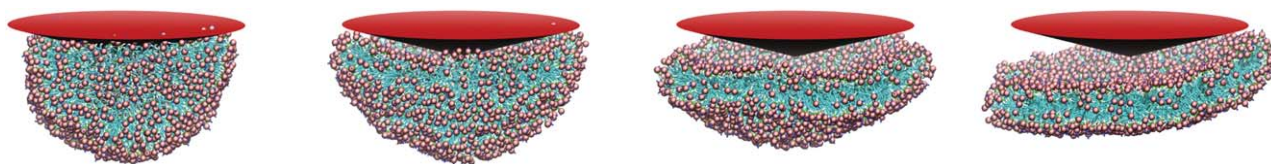


Fig. 6 Spontaneous transformation of a lipid vesicle fragment into a bicelle during the PMF computation at $\theta = 75^\circ$. The snapshots are taken, from left to right, at 0.5, 19, 40, and 65 ns of CG-MD simulation time. The red cone denotes the shape of the bias potential applied to the hydrophobic core of the vesicle.

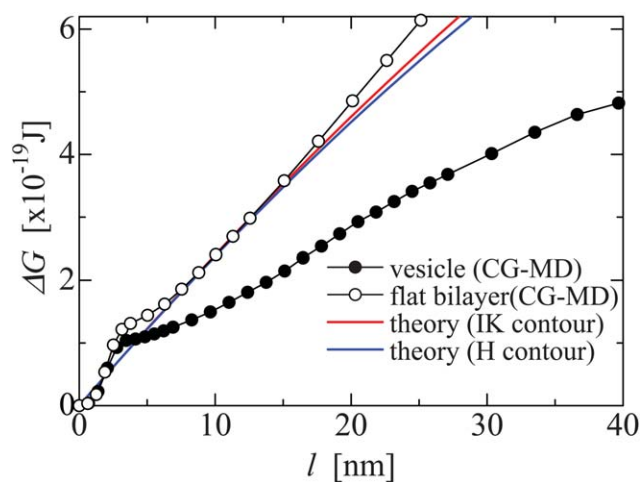


Fig. 8 Free energy change as a function of the line length of the bilayer rim. The line lengths were calculated as described in the main text. The theoretical lines are drawn by using eqn (1) with the Gaussian curvature modulus computed either using the IK or H contour. The error bars are smaller than the symbols.

length along the bilayer center is selected in this calculation, *i.e.*, $l = 2\pi \sin\theta(\rho(\theta) - t/2)$. Now the question is whether the difference in the free energy profiles between the vesicle and planar membranes can be explained by the bending free energy of the lipid bilayer or not. In Fig. 8, we also plot the free energy given by the Fromherz theory using the line tension and the Gaussian curvature modulus estimated from the CG-MD simulations of a planar DMPC membrane. The mean curvature modulus, $\kappa_c = 6.9 \times 10^{-20}$ J, is taken from our previous paper,⁶ where a Fourier analysis of the membrane height and thickness was carried out to evaluate the mean curvature modulus using the method proposed by Brannigan and Brown.³⁵ The calculated mean curvature modulus is in good agreement with that measured by pipette aspiration experiments for DMPC, 5.6×10^{-20} J,³⁶ though the experimental data available from other techniques are in the range of $5\text{--}15 \times 10^{-20}$ J.³⁷ Since we have two different values for $\bar{\kappa}$ depending on the choice of the integration contour of the pressure profile, we plotted two lines for the Fromherz theory corresponding to the two contour choices. Regardless of the contour, we find that the free energy reduction from the bending elasticity is too small to explain the difference of pore formation free energies between the vesicle and planar bilayers calculated from CG-MD. This strongly suggests that there is a free energy contribution not explicitly taken into account in the Fromherz theory that plays an important role in the vesicle-to-bicelle transformation. A plausible candidate to explain this discrepancy is the repartitioning of DMPC lipid molecules between the inner and outer leaflets of the bilayer membrane induced by the changing curvature of the vesicle fragment. We find 512 and 1000 DMPC molecules in the inner and outer leaflets of the vesicle, respectively. This changes to a symmetric partition of lipids in the two leaflets when transformed into the bicelle. Therefore a significant number of lipids migrate to the inner leaflet from the outer one during the vesicle opening process. This can be thought of as a relaxation of the interior structure of the membrane. Although Fromherz discussed this relaxation, his theory does not formally treat it

because the membrane is assumed to be an elastic sheet with zero thickness.³⁸ Even in MD simulations, the repartitioning of lipids between the two leaflets is prohibited when the pore is too small and still hydrophobic as mentioned in Sec. 3.1. For small pore sizes ($l < 3\text{--}4$ nm) we actually found that the CG-MD free energy slope is even steeper than the theoretical one. However, once the pore size reaches a large enough value to make a hydrophilic pore due to the lipid reorientation at the bilayer rim, the inner and outer leaflets of the vesicle membrane are connected to one another. Thus, the repartitioning of lipids between the two leaflets occurs easily at the bilayer rim, which contributes significantly to decrease the free energy cost to grow the pore in the vesicle.

In this paper, we investigated the free energy cost of a small DMPC vesicle to transform into a bicelle using a series of CG-MD simulations. Although there have been several studies reported of the pore formation free energy in planar membranes,^{39–42} to the best of our knowledge this is the first study to investigate the free energy barrier of a vesicle-to-bicelle transformation using MD simulations. We have found that the free energy needed to open a vesicle is much smaller than that to open a planar membrane. This may be intuitively explained by a continuum elastic membrane model proposed by Fromherz, where two energy terms; namely line tension and bending energy, are considered. However, our detailed analysis demonstrates that the bending energy contribution is too small to explain the difference of the pore formation free energies between the vesicle and the planar membranes. The repartitioning of DMPC lipids between the inner and outer leaflets of the vesicle membrane was proposed to lower the free energy barrier for the vesicle-to-bicelle transformation. Although this effect would be expected to be less important for giant vesicles, it should play a significant role in the small vesicle considered here. The use of CG-MD and a novel free energy procedure allowed us to conduct a stringent test of elastic theory and gain insight into the stability of small vesicles.

Acknowledgements

The authors thank Mike Klein, Russell DeVane, and Preston Moore for their useful discussion. This work is partly supported by JST-CREST, KAKENHI (No. 11004604), and the Next Generation Super Computing Project, Nanoscience Program, MEXT, Japan.

References

- 1 *Lipid Polymorphism and Membrane Properties*, ed. R. M. Epand, Academic Press, 1997, vol. 44.
- 2 J. Israelachvili, *Intermolecular & Surface Forces*, Academic Press, New York, 1992.
- 3 P. Fromherz, *Chem. Phys. Lett.*, 1983, **94**, 259–266.
- 4 U. Seifert, *Adv. Phys.*, 1997, **46**, 13–137.
- 5 S. J. Marrink, A. H. de Vries and D. P. Tieleman, *Biochim. Biophys. Acta, Biomembr.*, 2009, **1788**, 149–168.
- 6 W. Shinoda, R. DeVane and M. L. Klein, *J. Phys. Chem. B*, 2010, **114**, 6836–6849.
- 7 W. Shinoda, R. DeVane and M. L. Klein, *Mol. Simul.*, 2007, **33**, 27–36.
- 8 W. Shinoda, R. DeVane and M. L. Klein, *Soft Matter*, 2008, **4**, 2454–2462.
- 9 R. DeVane, W. Shinoda, P. B. Moore and M. L. Klein, *J. Chem. Theory Comput.*, 2009, **5**, 2115–2124.
- 10 M. L. Klein and W. Shinoda, *Science*, 2008, **321**, 798–800.

- 11 C.-C. Chiu, R. DeVane, M. L. Klein, W. Shinoda, P. B. Moore and S. O. Nielsen, *J. Phys. Chem. B*, 2010, **114**, 6394–6400.
- 12 R. Devane, M. L. Klein, C.-C. Chiu, S. O. Nielsen, W. Shinoda and P. B. Moore, *J. Phys. Chem. B*, 2010, **114**, 6386–6393.
- 13 N. Kucerka, S. Tristram-Nagle and J. Nagle, *J. Membr. Biol.*, 2005, **208**, 193–202.
- 14 G. J. Martyna, M. L. Klein and M. Tuckerman, *J. Chem. Phys.*, 1992, **97**, 2635–2643.
- 15 H. C. Andersen, *J. Chem. Phys.*, 1980, **72**, 2384–2393.
- 16 M. Parrinello and A. Rahman, *J. Appl. Phys.*, 1981, **52**, 7182–7190.
- 17 G. J. Martyna, M. E. Tuckerman, D. J. Tobias and M. L. Klein, *Mol. Phys.*, 1996, **87**, 1117–1157.
- 18 M. Allen and D. Tildesley, *Computer Simulation of Liquids*, Oxford, 1989.
- 19 W. Shinoda and M. Mikami, *J. Comput. Chem.*, 2003, **24**, 920–930.
- 20 <http://staff.aist.go.jp/w.shinoda/MPDyn/index.html>.
- 21 C.-C. Chiu, R. J. K. U. Ranatunga, D. T. Flores, D. V. Perez, P. B. Moore, W. Shinoda and S. O. Nielsen, *J. Chem. Phys.*, 2010, **132**, 054706.
- 22 A. Ben-Shaul, in *Handbook of Biological Physics*, ed. R. Lipowsky and E. Sackmann, Elsevier, 1995, vol. 1, ch. 7. *Molecular Theory of Chain Packing, Elasticity and Lipid-Protein Interaction in Lipid Bilayers*, pp. 359–399.
- 23 J. Sonne, F. Hansen and G. Peters, *J. Chem. Phys.*, 2005, **122**, 124903.
- 24 E. Karatekin, O. Sandre, H. Guitouni, N. Borghi and P. Puech, *Biophys. J.*, 2003, **84**, 1734–1749.
- 25 D. Zhelev and D. Needham, *Biochim. Biophys. Acta, Biomembr.*, 1993, **1147**, 89–104.
- 26 I. Genco, A. Gliozzi, A. Relini, M. Robello and E. Scalas, *Biochim. Biophys. Acta, Biomembr.*, 1993, **1149**, 10–18.
- 27 P. Fromherz, C. Röcker and D. Ruppel, *Faraday Discuss. Chem. Soc.*, 1986, **81**, 39–48.
- 28 L. Chernomordik, M. Kozlov, G. Melikyan, I. Abidor, V. Markin and Y. Chizmadzhev, *Biochim. Biophys. Acta, Biomembr.*, 1985, **812**, 643–655.
- 29 W. Harbich and W. Helfrich, *Z. Naturforsch.*, 1979, **34a**, 1063–1065.
- 30 C. Taupin, M. Dvolaitzky and C. Sauterey, *Biochemistry*, 1975, **14**, 4771–4775.
- 31 N. Srividya and S. Muralidharan, *J. Phys. Chem. B*, 2008, **112**, 7147–7152.
- 32 F. Jiang, Y. Bouret and J. Kindt, *Biophys. J.*, 2004, **87**, 182–192.
- 33 H. Leontiadou, A. Mark and S. Marrink, *Biophys. J.*, 2004, **86**, 2156–2164.
- 34 B. Hafskjold and T. Ikeshoji, *Phys. Rev. E: Stat. Phys., Plasmas, Fluids, Relat. Interdiscip. Top.*, 2002, **66**, 011203.
- 35 G. Brannigan and F. Brown, *Biophys. J.*, 2006, **90**, 1501–1520.
- 36 W. Rawicz, K. Olbrich, T. McIntosh, D. Needham and E. Evans, *Biophys. J.*, 2000, **79**, 328–339.
- 37 D. Marsh, *Chem. Phys. Lipids*, 2006, **144**, 146–159.
- 38 A possible extension of the Fromherz theory suggested in his original paper was to treat the bending moduli as a variable with respect to the reaction coordinate (order parameter),³ though it is obviously too difficult to determine the bending moduli experimentally except for a phenomenological fitting to the theory.
- 39 T. Tolpekina, W. D. Otter and W. Briels, *J. Chem. Phys.*, 2004, **121**, 8014–8020.
- 40 T. Tolpekina, W. D. Otter and W. Briels, *J. Chem. Phys.*, 2004, **121**, 12060–12066.
- 41 Z. Wang and D. Frenkel, *J. Chem. Phys.*, 2005, **123**, 154701.
- 42 J. Wohlert, W. den Otter, O. Edholm and W. Briels, *J. Chem. Phys.*, 2006, **124**, 154905.